Arab J Sci Eng (2018) 43:4303–4313
https://doi.org/10.1007/s13369-017-2961-9

RESEARCH ARTICLE - SPECIAL ISSUE - COMPUTER ENGINEERING AND COMPUTER SCIENCE

Homomorphic Normalization-Based Descriptors for Texture Classification

Sonali Dash[1] · **Uma Ranjan Jena**[1] · **Manas Ranjan Senapati**[2]

Received: 14 March 2017 / Accepted: 5 November 2017 / Published online: 20 November 2017

Abstract Illumination variation is an essential trait in texture analysis, since the same texture can be surrounded with different illuminations, which can greatly affect the classification rate. This paper introduces a new approach to extract the texture features applying illumination normalization-based texture descriptors. The prime objective is to enhance the classification accuracy by normalizing the illumination of colour textures. Normalization of illumination is achieved by applying homomorphic filter. For feature extraction, two relevant approaches grey-level co-occurrence matrix (GLCM) and Laws' mask are utilized. Experiments are conducted for normalized co-occurrence and Laws' filter for colour images. Classification rates of the traditional GLCM and Laws' mask descriptors are included for baseline comparison. The effectiveness of the introduced techniques is assessed on three benchmark texture datasets, i.e. STex, VisTex, and ALOT. A k-nearest neighbour (k-NN) classifier is utilized to perform texture classification. Results show that the proposed approach has achieved higher classification rates and outperformed existing methods.

Keywords Texture · Colour · Laws' mask · GLCM · Homomorphic filter · Classification

✉ Manas Ranjan Senapati
manassena@gmail.com

Sonali Dash
sonali.isan@gmail.com

Uma Ranjan Jena
urjena@rediffmail.com

[1] Department of Electronics and Tele-Communication Engineering, VSSUT, Burla 768018, Odisha, India

[2] Department of Information Technology, VSSUT, Burla 768018, Odisha, India

1 Introduction

In image analysis, texture and colour are two widely accepted important properties of images. Many authors have proposed various texture feature extractions and classification techniques for grey texture images, while ignoring the colour information. Considering the colour information, classification rate can be enhanced, as colour is the most essential element especially when associated with real-world images. A pattern surrounded by chromatic and structural distribution can be considered as a colour texture. In 1993, Tan and Kittler have applied discrete cosine transform for the extraction of texture features from grey images, while features extracted from colour histograms are applied for colour explanation [1]. In 2000, to classify the defective parquet slabs Kyllonenan and Pietikainen have calculated the texture features by combining Local Binary Patterns (LBP) features with colour histogram features [2]. In 2001, Drimbarean and Whelan have recommended the classification of colour texture images by utilizing the grey texture descriptors, and then extended for feature extraction of the colour images. They have mentioned two alternatives for the extraction of features in colour texture analysis. The first one is by employing grey-level texture analysis, features are derived separately from each colour band and then combining the results of channel-wise operations. The second is deriving textural details from luminance plane together with pure chrominance features [3]. In 2002, Palm and Lehmann [4] have proposed colour texture classification by using Gabor filter. In 2004, Palm has combined colour and texture using co-occurrence matrices and reported in improvement of classification accuracy [5]. In 2005, Arivazhagan et al. [6] have recommended colour texture classification using Wavelet Statistical Features (WSF) and Wavelet Co-occurrence Features (WCF). In 2011, Arivazhagan et al. [7] have also suggested colour

texture image classification using wavelet texture spectral features. In 2016, Dey et al. have recommended colour image retrieval scheme in which the colour and texture features are extracted separately by employing red, green, blue (RGB) colour histogram and discrete wavelet transform (DWT) through local extrema peak valley pattern (LEPVP). For the enhancement of retrieval rate, they have combined the colour features with texture features [8].

For any kind of texture classification methods, texture feature descriptors are vital in texture analysis. Many authors have proposed various types of texture descriptors. Few examples of local texture descriptors are GLCM, Laws' mask, and LBP have gained popularity in the field of texture analysis [9–11]. Several multiresolution and multichannel transform methods have also been proposed for texture analysis such as wavelet frame transform, Gabor filters, and dyadic wavelet transform [12–14]. Further study illustrates that authors have also introduced hybrid models to achieve better classification rate. For example, multiscale grey-level co-occurrence matrices [15], multiresolution LBP [16], Gaussian image pyramid-based texture features [17], and texture classification using steerable pyramid-based Laws' masks [18] for grey-level texture classification.

Over the last few years, many researchers have addressed the problem of illumination variance. Illumination preprocessing technique tries to control the variation and produces more stable images under illumination changes. Normalization can be achieved through image transformation of image or else by synthesizing using some normalization techniques. Then these normalized images are adopted for classification. There are many existing techniques available to deal with the illumination variation problem. Du and Ward [19] have suggested a new approach of histogram equalization (HE) in which HE is applied to the low frequency and emphasizes on the high frequency components for face recognition. Jobson et al. [20] have recommended multiscale retinex (MSR) approach for illumination normalization, in which low frequency information is cancelled by dividing the image by a smoothed version of itself. Delac et al. [21] have proposed an illumination normalization method based on homomorphic filtering technique to enhance the facial recognition with challenging illumination conditions. Wang et al. have suggested wavelet-based illumination normalization approach using eigen face for face recognition [22]. Chen et al. [23] have recommended an illumination normalization method utilizing Discrete Cosine Transform (DCT) for face recognition. Xie and Lam have applied local normalized technique for illumination normalization on face database and concluded with high recognition rates [24]. Emadi et al. have proposed illumination normalization using 2D wavelet for face verification and reported high verification performance [25]. Tan and Triggs have used normalization technique for the enhancement of local texture features for face recognition. For illumination normalization in preprocessing stage Gamma correction, Difference of Gaussian filtering, Masking (optional) and Contrast equalization have been used. Local Ternary Pattern (LTP) and Gabor filter are employed to extract the features [26]. More recently, Fan and Zhang have implemented illumination normalization technique through homomorphic filtering and histogram equalization for the recognition of face [27]. The literature study has revealed that recognition rate can be improved using illumination normalization techniques. Despite the fact that there are several illumination normalization methods proposed for the analysis of human faces, but hardly there is any work done on normalization of texture images and analysis.

Even though colour is the most important attribute, as well it is highly exposed to the illumination under which image content captured is varied. Variation in illumination is one of the greatest aspects restricting the accomplishment of texture classification. In general, the texture of an image is associated with the intensity variation in the image plane, and as such contains information regarding contrast, uniformity, regularity, etc. Coarseness and directionality are the two main features for defining a texture. Image variance is linearly related to the surface variance. Any variation in illuminant tilt can change the directional properties of image texture, while variation in illuminant slant can disturb the image variance. Both of these effects have a great impact in texture measures. Normalization reduces the variation of the features due to change in illumination. Therefore, it is expected that normalization of images will reduce the classification error rate. Most of the texture analysis methods are responsive to illumination variations. Some authors have stated their views regarding effect of illumination in colour texture analysis, and recommended some approaches. Brief reviews on these are discussed. In 2004, Maenpaa and Pietikainen have suggested two different techniques for the analysis of colour texture: firstly, colour and texture are processed separately, and secondly both are considered jointly. They have concluded that combining colour information with texture measures improves the accuracy, provided the condition of illumination is static. On the other hand, in varying illumination, grey-scale texture performs superior to colour texture [28]. In 2009, Burghouts and Geusebroek have recommended material-specific adaption of colour invariant features. They have constructed colour invariant filter sets from the original MR8 filter bank and evaluated their approach on CURET and ALOT datasets including clutter. They have modified MR8 filter bank in different ways to normalize the colour channels [29]. In 2012, Vacha and Haindl [30] have proposed a texture recognition method through robust Markovian features and demonstrated the influence of CAR (Causal Autoregressive Random) illumination invariant Markovian features on ALOT dataset in addition to other datasets.

Even though there are so many methods for colour texture analysis, but to improve the colour texture classification based on illumination normalization by utilizing the traditional texture feature descriptors are still unexplored. Thus, this work recommends the extension of GLCM and Laws' mask to be more robust under illumination variations. Homomorphic filter is utilized for illumination normalization. First, illumination normalization is carried out using homomorphic filter at different values of high frequency gain (γ_H), and low frequency gain (γ_L) in each channel separately of RGB component. For texture features extraction, we have used two traditional approaches, i.e. co-occurrence and Laws' mask. Colour texture features are extracted separately from RGB colour panel. The same procedure is also followed for GLCM. Simple k-NN classifier is used for the classification. To verify our proposed method, we have taken VisTex, STex and ALOT, the three colour texture datasets. The results demonstrate the improvement of classification rates when compared with the original methods. The paper is arranged as follows: Sect. 2 discusses about the theoretical background of homomorphic filter, co-occurrence, Laws' mask, and k-NN classifier. Section 3 explains in detail about various techniques of the proposed method. Finally, Sect. 4 reports the outcome of experiments. Then, conclusions are drawn.

2 Theoretical Background

2.1 Homomorphic Filter

One of the commonly used methods for enhancing the uneven illumination images is homomorphic filtering. This approach is based on the design of illumination-reflectance model. Mathematically, an image can be modelled in terms of illumination$L(x, y)$ and reflectance$R(x, y)$. Then, the image $I(x, y)$ is defined as

$$I(x, y) = L(x, y) * R(x, y) \tag{1}$$

Usually, the illumination part is considered by slow spatial variations and the reflectance part is tending to change suddenly at the junctions of distinct images. These individualities of the two components relate the low frequencies of the Fourier transform of the logarithm image with illumination and high frequencies with reflectance. To compensate for the non-uniform illumination, the low frequency component must be attenuated to some degree and high frequency component must be retained. This can be obtained by transforming the images into frequency domain, and then performing the filtering process in frequency domain. The illumination and reflectance components can be controlled by homomorphic filter using filter function. The filter function affects the control of low frequency and high frequency elements of the Fourier transformed images in different manners. Generally, homomorphic filtering can be executed with following five stages.

STAGE 1: Apply logarithm function to transform the multiplicative components to additive components. STAGE 2: For the frequency domain transformation take Fourier transform of the image. STAGE 3: The resultant transformed image is processed by means of filter function. STAGE 4: Generate the filtered image in the spatial domain by taking an inverse Fourier transform. STAGE 5: Lastly, take the exponential function to invert the log transform and to get the enhanced image $g(x, y)$. The five sets of equation that represent the homomorphic filter are specified as follows.

$$z(x, y) = lnL(x, y) + lnR(x, y) \tag{2}$$

$$Z(u, v) = F_L(u, v) + F_R(u, v) \tag{3}$$

$$S(u, v) = H(u, v) F_L(u, v) + H(u, v) F_R(u, v) \tag{4}$$

$$s(x, y) = \Im^{-1}\{H(u, v) F_L(u, v) + H(u, v) F_R(u, v)\} \tag{5}$$

$$g(x, y) = \exp\{s(x, y)\} \tag{6}$$

In the literatures, there are several variations for the filter function $H(u, v)$. The modified version of Gaussian high-pass filter, named as Difference of Gaussian filter (DoG) is given as below.

$$H(u, v) = (\gamma_H - \gamma_L)\left[1 - \exp\left\{c\left(\frac{D(u, v)}{D_0}\right)^2\right\}\right] + \gamma_L \tag{7}$$

where constant c is the steepness control, D_0 is the cutoff frequency, $D(u, v)$ is the distance from the origin of the centred Fourier transform and γ_H, γ_L are the high frequency and low frequency gain, respectively. The enhancement approach using this concept is summarized in Fig. 1.

2.2 Laws' Mask Method

Laws has established a set of two-dimensional masks and named it as Laws' masks [10]. The main purpose of this approach is to create some specific masks from the combination of one dimensional kernel vector. Then, these masks are used for filtering of images to evaluate the texture properties. There are five types of one dimensional kernel of length five those are: h1 = [1 4 6 4 1], h2 = [−1 −2 0 2 1], h3 = [−1 0 2 0 −1], h4 = [−1 2 0 −2 −1], and h5 = [1 −4 6 −4 1]. The five types of vectors correspond to level, edge, spot, wave, and ripple, respectively. Using this scheme, 25 two-dimensional different masks are created through convolution of each ver-

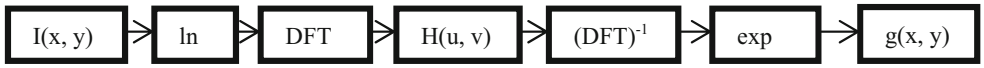

Fig. 1 The flow chart of Homomorphic filtering

tical vector with horizontal one. These specific masks are used for identifying the behaviour of texture.

2.3 Grey-Level Co-occurrence Matrix

A method of extracting textural details relating to grey-level transition between two pixels utilizes co-occurrence matrix, and initially has introduced fourteen statistical features [9]. GLCM has been proved to be a valuable method for image texture analysis. This matrix represents the joint distribution of grey-level pairs of neighbouring pixels. According to different distances and angles, a number of co-occurrence matrices can be created. Thus, different information can be achieved by varying the spatial relationship. Co-occurrence matrix can be represented as two-dimensional array X. Within this matrix, both rows and columns indicate a set of probable image values M. For instance, grey-level images M can be the set of possible grey levels and for colour images, M can be set of feasible colours. The significance of $X(m, n)$ is that it specifies the occurrence of m with reference to n with certain selected spatial relationship. The normalized grey tone co-occurrence matrix is represented as $\sum_m \sum_n (m - \mu_m)(n - \mu_n) P_d(m, n) \sigma_m \sigma_n$,

$$P_d(m, n) = \frac{X_d(m, n)}{\sum_m \sum_n X_d(m, n)} \tag{8}$$

The followings features are derived from a normalized co-occurrence matrix.

$$\text{Energy} = \sum_m \sum_n P_d^2(m, n) \tag{9}$$

$$\text{Entropy} = -\sum_m \sum_n P_d(m, n) log_2 P_d(m, n) \tag{10}$$

$$\text{Contrast} = \sum_m \sum_n (m - n)^2 P_d(m, n) \tag{11}$$

$$\text{Homogeneity} = \sum_m \sum_n \frac{P_d(m, n)}{1 + |m - n|} \tag{12}$$

$$\text{Correlation} = \frac{\sum_m \sum_n (m - \mu_m)(n - \mu_n) P_d(m, n)}{\sigma_m \sigma_n} \tag{13}$$

where μ_m, μ_n are the means and σ_m, σ_n are the standard deviations of the rows and columns and are defined as follows.

$$\mu_m = \sum_m m P_d(m) \tag{14}$$

$$\mu_n = \sum_n n P_d(n) \tag{15}$$

$$\sigma_m^2 = \sum_m (m - \mu_m)^2 P_d(m) \tag{16}$$

$$\sigma_n^2 = \sum_n (n - \mu_n)^2 P_d(n) \tag{17}$$

2.4 k-Nearest Neighbour (k-NN) Classifier

In this work, k-NN classifier is used for image texture classification. The k-NN algorithm is a technique for classifying objects based on closest training examples in the feature space. The classification process divides data into a test set and a training set. Object classification is dependent on maximum votes of its neighbours and allotted to the class that is most common among its k-nearest neighbours. For classification, if $k = 1$, then the object picks the nearest neighbour that means the patterns which are nearer to each other in the feature space are likely to belong to the similar pattern class. This k-nearest neighbours are selected by using some predefined distance metric to compute and select the nearest training patterns that are neighbours to input sample in the sense of the selected metric. Precisely, k-NN classifier classifies the new query instance based on a similarity measure. Various types of distance measure approaches can be used such as Euclidean, City block, Cosine and Mahalanobis distance. Even though k-NN classification method gives good classification accuracy, still it is very sensitive to noise data [31]. The value of k should be odd to avoid ties. The larger the value of k, the lesser is the influence of noise on the classification [32]. Tenfold cross-validation can also be employed for classification to obtain more accurate validation [33]. In our work, initially the features are normalized to avoid the wide range of variations, and then classification is performed based on train and test validation for each dataset following the k-NN rule. The datasets (STex, VisTex), which are used in the experiments are captured under real-world conditions and possibly may contain some inherent noise. Therefore, $k = 5$ is chosen for the nearest neighbour classifier.

3 Proposed Methodology

This work recommends enhancing of the colour texture images by illumination normalization through homomorphic filter and then the texture features are extracted by employing Laws' mask and co-occurrence methods. This section outlines the colour space, homomorphic parameter selection, the experimental set-up used for feature extraction and classification.

3.1 Colour Space

In colour images, RGB is perhaps the most common format. The RGB space contains three colour components, red, green and blue. In our experiment, we have used RGB colour plane, the colour texture images are divided into three subimages in the colour channel of R, G and B. The texture features are extracted separately from individual colour channel using traditional texture descriptors and afterwards the results of each channel are combined. Although this is a simple technique, it performs well.

3.2 Parameter Selection of Homomorphic Filter

Generally, all the parameters D_0, γ_H and γ_L of homomorphic filter are determined experimentally and there is not much theoretical basis on selecting the exact suitable values for these parameters. The high frequency and low frequency components of homomorphic filter must follow the condition $\gamma_H > \gamma_L \geq 0$. If too small values are selected for γ_L then it may omit the soft edge and detail information. Conversely, too large values of γ_H may increase the noise contains in high frequencies. Therefore, values of γ_H and γ_L are often selected experimentally. As we are working only with the textural images, so almost at everywhere, the textures of foreground and background images are much alike and there is no abrupt change. Hence, the parameters are selected as follows.

a. Initially set $\gamma_H = 1$ and γ_L varying from 0 to 1.
b. Then set $\gamma_H = 1.5$ and γ_L varying from 0 to 1.
c. Then set $\gamma_L < \gamma_H < 1$ and γ_L varying from 0 to 1.

Once the parameters are selected, then homomorphic filter is implemented on the input images following the 5 stages as described in Sect. 2.1 to obtain the normalized images.

3.3 Experimental Set-up for Feature Extraction and Classification

To validate the efficacy of the suggested method for texture feature extraction, two traditional approaches GLCM and Laws' mask methods are utilized. The different experiments carried out are as follows.

a. The first experiment is conducted only for conventional Laws' mask descriptor. Individually, the three colour components (RGB) of colour texture images are passed through Laws' mask descriptors having 25 numbers of masks. Both training and testing images are convolved with twenty-five numbers of masks. The convolved outputs are then passed through three different energy measurement filters. The three energy measurement filters are described as follows:

$$\text{Mean} = \frac{\sum_N \text{Neighbouringpixels}}{N} \tag{18}$$

$$\text{Absolute mean} = \frac{\sum_N abs\ (\text{Neighbouringpixels})}{N} \tag{19}$$

$$\text{Standard deviation} = \sqrt{\frac{\sum_N (\text{Neighbouringpixels} - \text{mean})^2}{N}} \tag{20}$$

where N represents the window size. Then, outputs of energy measurement filters are normalized by min–max normalization method and then the statistical features are extracted. Statistical features like absolute mean, energy and entropy are extracted for three colour components R, G and B are defined as follows.

$$\text{ABSM} = \frac{1}{PQ} \sum_{a=1}^{P} \sum_{b=1}^{Q} |I\ (a, b)| \tag{21}$$

$$\text{Energy} = \frac{1}{PQ} \sum_{a=1}^{P} \sum_{b=1}^{Q} I^2\ (a, b) \tag{22}$$

$$\text{Entropy} = \frac{1}{PQ} \sum_{a=1}^{P} \sum_{b=1}^{Q} I\ (a, b)\ (-ln I\ (a, b)) \tag{23}$$

where $I\ (a, b)$ is the pixel value, and P and Q are image dimensions. Then, all the features obtained from the three colour channels are concatenated.

b. The second experiment is conducted through co-occurrence approach. GLCM is applied individually to the three colour components of colour texture images. From co-occurrence matrix eight numbers of statistical features, mean, variance, standard deviation, energy, entropy, contrast, homogeneity and correlation are extracted. All the features of three colour channels are then concatenated before classification.
c. In the third set-up, we have conducted the experiments for our proposed methods. Different values of γ_H and γ_L are applied to homomorphic filter (as mentioned in Sect. 3.2) individually to the three channels R, G, and B of colour texture images. Then, combine all these three colour components to get the normalized colour images. These normalized images are then passed through the conventional Laws' mask descriptor followed by experiment number a, and co-occurrence approach followed by experiment number b to obtain the texture features.

In the experiments, k-NN classifier is adopted in the task of classification as described in Sect. 2.4. The procedural steps involved are shown in block diagram Fig. 2.

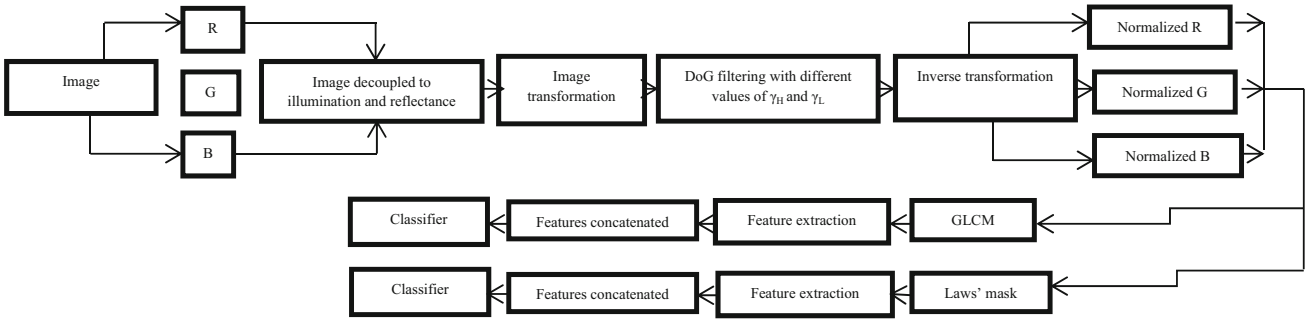

Fig. 2 Block diagram of the proposed method

Fig. 3 STex database

4 Experimental Results, Comparison and Discussion

The verification of the recommended illumination normalized descriptors is performed using three colour databases VisTex, STex and ALOT. Comparative experiments of classification by using Laws' mask, co-occurrence and our proposed method illumination normalized descriptors are given. The experiments carried out, and the results of each database are discussed below.

4.1 STex Database

The Salzburg Texture Image Database (STex) is a huge set of 476 colour images that have been acquired nearby Salzburg, Austria [34]. Inside the STex dataset, the great majority of texture images are stationary and have more chromatic richness than VisTex. Twenty-five texture images (512 × 512pixels), as shown in Fig. 3, are chosen from STex database. Each image is divided into non-overlapping size of 128 × 128 pixels. Both training and testing sets, each of which include 200 images. The traditional Laws' mask has delivered classification accuracy of 87.00% for the mean filter, 72.50% for the absolute mean filter, and 72.00% for the standard deviation filter. Among all the proposed homomorphic normalized Laws' mask approach the maximum classification accuracy of 92.00% is obtained for the mean filter at $\gamma_H = 0.7$ and $\gamma_L = 0.5$. The second highest classification accuracy of 91.00% is obtained at $\gamma_H = 0.6$ and $\gamma_L = 0.5$. The third best classification accuracy of 89.50% is achieved at $\gamma_H = 0.8$ and $\gamma_L = 0.5$. Also for some other values such as $\gamma_H = 1$ and γ_L varying from 0 to 1 higher classification accuracies are obtained for the mean filter. Similarly, highest classification accuracy of 83.50% for the absolute mean filter and 84.50% for the standard deviation filter are obtained at a value of $\gamma_H = 0.6$ and $\gamma_L = 0.5$. The conven-

Fig. 4 VisTex database

Fig. 5 ALOT database

Table 1 Classification results of conventional Laws' masks descriptor (5 × 5) for colour images

Different databases	No. of features for each image	Classification accuracy (%)		
		Mean	Absolute mean	SD
STex dataset	225	87.00	72.50	72.00
VisTex dataset	225	65.00	60.50	59.50
ALOT dataset	225	98.50	97.33	96.67

Table 2 Classification results of conventional GLCM descriptor for colour images

Different databases	No. of features for each image	Classification accuracy (%)
STex dataset	30	56.50
VisTex dataset	30	59.50
ALOT dataset	30	87.00

tional co-occurrence approach has delivered classification accuracy of 56.50%. Among all the proposed homomorphic normalized co-occurrence approach the highest classification accuracy of 76.00% is obtained from a combination of $\gamma_H = 0.6$ and $\gamma_L = 0.5$. The second highest classification accuracy of 75.50% is achieved for $\gamma_H = 0.7$ and $\gamma_L = 0.5$. The third best classification accuracy of 73.50% is obtained for $\gamma_H = 0.8$ and $\gamma_L = 0.5$. At the value $\gamma_H = 1$

Table 3 Performance evaluations of normalized homomorphic filter Laws' mask descriptor for colour texture images with different combinations of γ_H and γ_L.

Normalized features	No. of features	Classification accuracy (%)		
		Mean	Absolute mean	SD
STex dataset				
Laws' masks ($\gamma_H = .6, \gamma_L = .5$)	225	91.00	**83.50**	**84.50**
Laws' masks ($\gamma_H = .7, \gamma_L = .5$)	225	**92.00**	76.00	79.50
Laws' masks ($\gamma_H = .8, \gamma_L = .5$)	225	89.50	75.00	78.00
Laws' masks ($\gamma_H = .9, \gamma_L = .5$)	225	88.50	74.00	77.00
Laws' masks ($\gamma_H = 1, \gamma_L = .2$)	225	87.00	70.00	73.50
Laws' masks ($\gamma_H = 1, \gamma_L = .3$)	225	87.50	70.50	75.00
Laws' masks ($\gamma_H = 1, \gamma_L = .4$)	225	87.50	70.50	75.00
Laws' masks ($\gamma_H = 1, \gamma_L = .5$)	225	88.00	72.50	74.50
Laws' masks ($\gamma_H = 1, \gamma_L = .8$)	225	87.50	72.50	74.50
Laws' masks ($\gamma_H = 1.5, \gamma_L = .5$)	225	74.00	60.50	61.00
Laws' masks ($\gamma_H = 1.5, \gamma_L = .8$)	225	73.00	60.00	62.00
VisTex dataset				
Laws' masks ($\gamma_H = .6, \gamma_L = .5$)	225	**70.50**	**68.00**	**66.50**
Laws' masks ($\gamma_H = .7, \gamma_L = .5$)	225	**70.50**	67.00	64.50
Laws' masks ($\gamma_H = .8, \gamma_L = .5$)	225	67.50	62.50	61.50
Laws' masks ($\gamma_H = .9, \gamma_L = .5$)	225	66.00	61.50	61.00
Laws' masks ($\gamma_H = 1, \gamma_L = .2$)	225	65.50	61.00	60.50
Laws' masks ($\gamma_H = 1, \gamma_L = .3$)	225	64.00	60.00	56.50
Laws' masks ($\gamma_H = 1, \gamma_L = .4$)	225	64.00	60.00	56.50
Laws' masks ($\gamma_H = 1, \gamma_L = .5$)	225	64.50	63.00	59.50
Laws' masks ($\gamma_H = 1, \gamma_L = .8$)	225	64.00	61.00	60.50
Laws' masks ($\gamma_H = 1.5, \gamma_L = .5$)	225	60.00	56.50	56.50
Laws' masks ($\gamma_H = 1.5, \gamma_L = .8$)	225	60.00	56.50	54.00
ALOT dataset				
Laws' masks ($\gamma_H = .6, \gamma_L = .5$)	225	98.67	97.00	95.67
Laws' masks ($\gamma_H = .7, \gamma_L = .5$)	225	99.00	97.00	95.67
Laws' masks ($\gamma_H = .8, \gamma_L = .5$)	225	99.00	96.83	96.17
Laws' masks ($\gamma_H = .9, \gamma_L = .5$)	225	98.77	96.50	96.00
Laws' masks ($\gamma_H = 1, \gamma_L = .2$)	225	98.83	96.00	96.50
Laws' masks ($\gamma_H = 1, \gamma_L = .3$)	225	98.67	95.83	96.50
Laws' masks ($\gamma_H = 1, \gamma_L = .4$)	225	98.67	95.83	96.50
Laws' masks ($\gamma_H = 1, \gamma_L = .5$)	225	**99.17**	96.33	**97.00**
Laws' masks ($\gamma_H = 1, \gamma_L = .8$)	225	98.83	97.33	96.67
Laws' masks ($\gamma_H = 1.5, \gamma_L = .5$)	225	95.50	92.00	91.50
Laws' masks ($\gamma_H = 1.5, \gamma_L = .8$)	225	94.50	91.50	91.33

Bold values indicate the improved classification rates by integrating homomorphic filter with traditional Laws' mask descriptor for three colour texture databases

Table 4 Performance evaluations of normalized Homomorphic filter GLCM descriptor for colour texture images with different combinations of γ_H and γ_L

Normalized features	No. of features	Classification accuracy (%)
STex dataset		
GLCM (γ_H = .6, γ_L = .5)	30	**76.00**
GLCM (γ_H = .7, γ_L = .5)	30	75.50
GLCM (γ_H = .8, γ_L = .5)	30	73.50
GLCM (γ_H = .9, γ_L = .5)	30	73.00
GLCM (γ_H = 1, γ_L = .2)	30	70.50
GLCM (γ_H = 1, γ_L = .3)	30	71.00
GLCM (γ_H = 1, γ_L = .4)	30	71.00
GLCM (γ_H = 1, γ_L = .5)	30	66.00
GLCM (γ_H = 1, γ_L = .8)	30	59.50
GLCM (γ_H = 1.5, γ_L = .5)	30	52.00
GLCM (γ_H = 1.5, γ_L = .8)	30	51.00
VisTex dataset		
GLCM (γ_H = .6, γ_L = .5)	30	**66.50**
GLCM (γ_H = .7, γ_L = .5)	30	65.50
GLCM (γ_H = .8, γ_L = .5)	30	66.00
GLCM (γ_H = .9, γ_L = .5)	30	66.00
GLCM (γ_H = 1, γ_L = .2)	30	64.00
GLCM (γ_H = 1, γ_L = .3)	30	63.00
GLCM (γ_H = 1, γ_L = .4)	30	63.00
GLCM (γ_H = 1, γ_L = .5)	30	62.00
GLCM (γ_H = 1, γ_L = .8)	30	58.50
GLCM (γ_H = 1.5, γ_L = .5)	30	50.50
GLCM (γ_H = 1.5, γ_L = .8)	30	49.50
ALOT dataset		
GLCM (γ_H = .6, γ_L = .5)	30	90.00
GLCM (γ_H = .7, γ_L = .5)	30	90.13
GLCM (γ_H = .8, γ_L = .5)	30	**91.00**
GLCM (γ_H = .9, γ_L = .5)	30	90.00
GLCM (γ_H = 1, γ_L = .2)	30	90.33
GLCM (γ_H = 1, γ_L = .3)	30	90.33
GLCM (γ_H = 1, γ_L = .4)	30	90.33
GLCM (γ_H = 1, γ_L = .5)	30	88.17
GLCM (γ_H = 1, γ_L = .8)	30	87.33
GLCM (γ_H = 1.5, γ_L = .5)	30	73.00
GLCM (γ_H = 1.5, γ_L = .8)	30	71.00

Bold values indicate the improved classification rates by integrating homomorphic filter with traditional GLCM descriptor for three colour texture databases

and γ_L varying from 0 to 1 higher classification accuracies are also achieved for the proposed homomorphic normalized co-occurrence method.

4.2 VisTex Database

In the second database, twenty-five natural (512 × 512 pixels) colour images with distinct view points and illumination

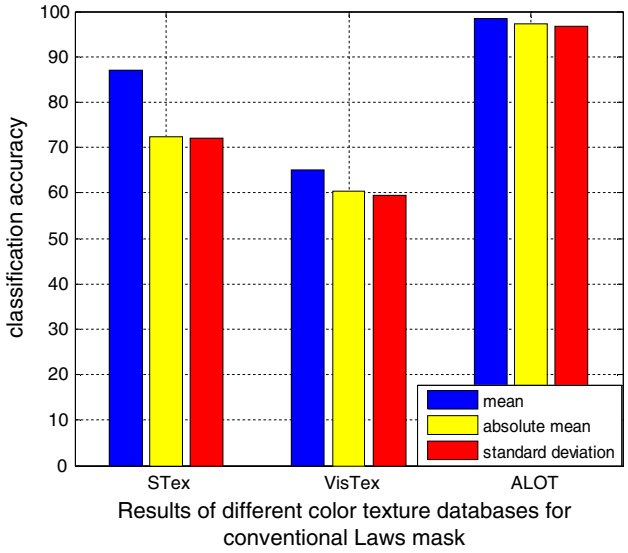

Fig. 6 Results of Original Laws' mask

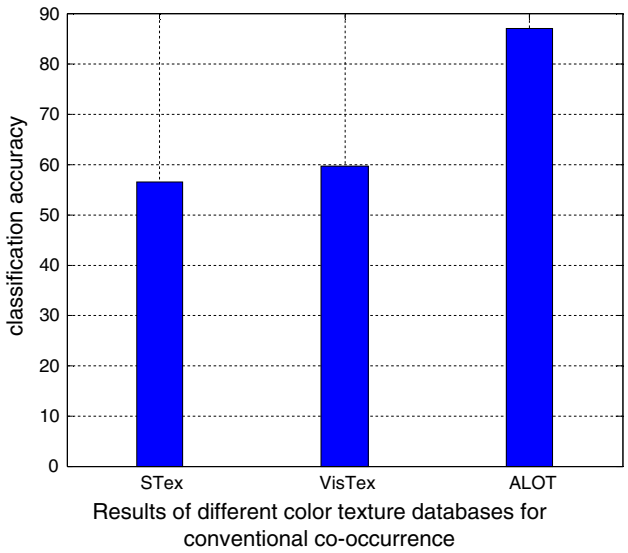

Fig. 7 Results of Original co-occurrence

orientations are selected as shown in Fig. 4 [35]. All the images are divided into non-overlapping subimages of size 128 × 128 pixels, and a database of 400 samples is created. From which 200 samples are used each for training and testing. The traditional Laws' mask has produced classification accuracy of 65.00% for the mean filter, 60.50% for the absolute mean filter and 59.50% for the standard deviation filter. The proposed homomorphic normalized Laws' mask approach for the mean filter has provided the highest classification accuracy of 70.50% at two different values, i.e. at $\gamma_H = 0.7$ and $\gamma_L = 0.5$, and at $\gamma_H = 0.6$ and $\gamma_L = 0.5$. The second highest classification accuracy of 67.50% is obtained with value at $\gamma_H = 0.8$ and $\gamma_L = 0.5$. The third highest classification accuracy of 66.00% is obtained from $\gamma_H = 0.9$ and $\gamma_L = 0.5$. When

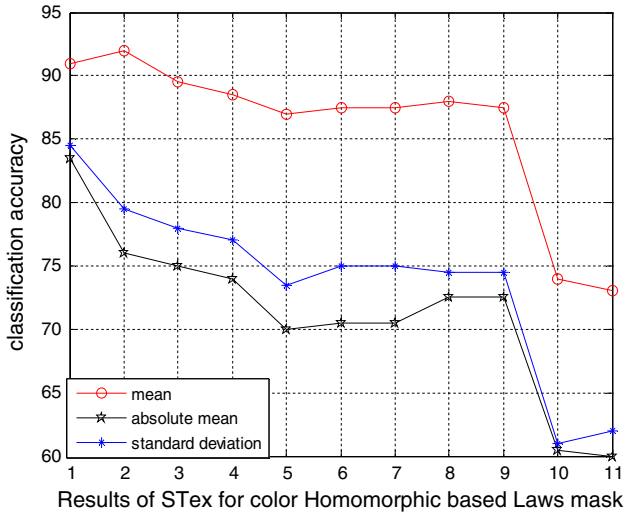

Fig. 8 Results of Homomorphic Law on STex.

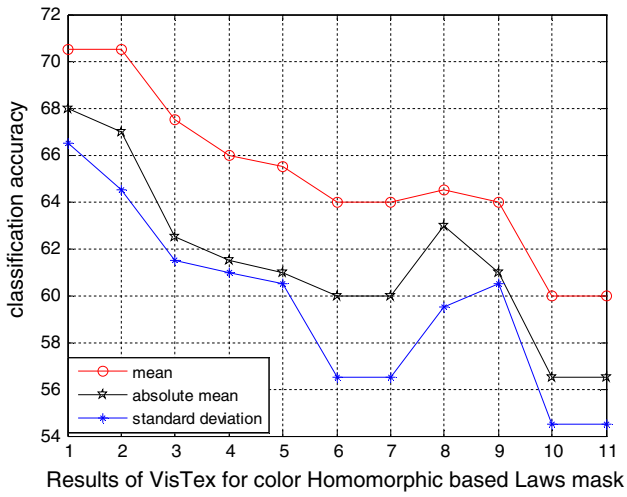

Fig. 9 Results of Homomorphic

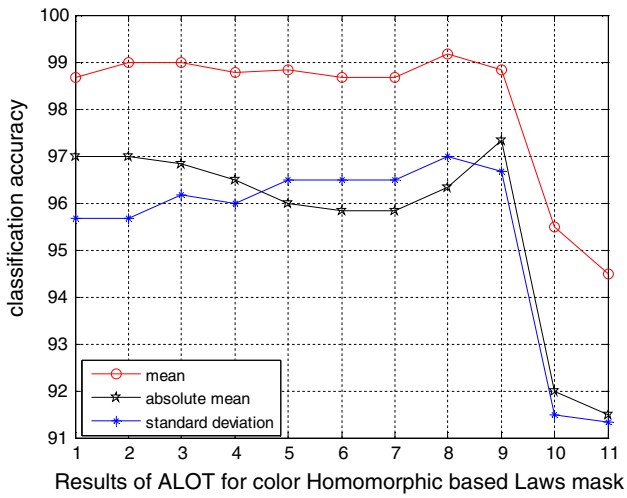

Fig. 10 Results of Homomorphic

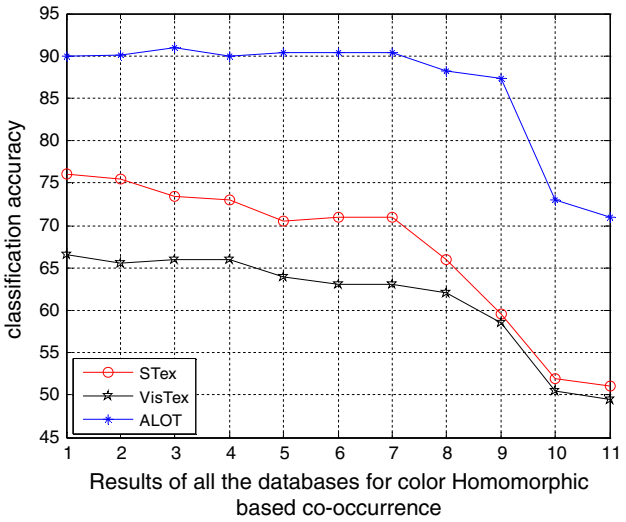

Fig. 11 Results of Homomorphic Law on VisTex. Law on ALOT. co-occurrence for all the databases

$\gamma_H = 1$ and γ_L varying from 0 to 1 higher classification accuracy of 65.50% is obtained only at $\gamma_L = 0.2$ on this database. For rest of all the values of γ_L lower classification accuracies are achieved for the mean filter. Highest classification accuracy of 68.00% for the absolute mean filter and 66.50% for the standard deviation filter are achieved correspondingly at the value of $\gamma_H = 0.6$ and $\gamma_L = 0.5$. The conventional co-occurrence approach has achieved classification accuracy of 59.50%. Among all the proposed homomorphic normalized co-occurrence approach maximum classification rate of 66.50% is achieved for value at $\gamma_H = 0.6$ and $\gamma_L = 0.5$. The second highest classification accuracy of 66.00% is obtained for two different values, i.e. at $\gamma_H = 0.9$ and $\gamma_L = 0.5$, and at $\gamma_H = 0.8$ and $\gamma_L = 0.5$. The third best classification rate of 65.50% is obtained at $\gamma_H = 0.7$ and $\gamma_L = 0.5$. It is also observed that for the values of $\gamma_H = 1$ and γ_L varying from 0 to 1 higher classification accuracies are obtained at all the values of γ_L for the normalized co-occurrence method.

4.3 ALOT Database

ALOT is an interesting colour database in which 250 distinct classes of rough textures are available, and each class consists of 100 samples. Four different cameras are used for the acquisition of images [36]. Six different illuminations (L = 1, 2, 3, 4, 5, 8) with four rotated angles ($R = 0^0, 60^0, 120^0, 180^0$) are acquired from each camera for individual image. Figure 5 represents 10 classes of texture images from ALOT database (size 384 × 256), and each class contains 20 different samples. Split the images into six 128 × 128 non-overlapping samples. As a result there are total 1200 samples are available. Each train and test sets contain 600 samples. The

Table 5 The graphical presentations of classification accuracies drawn for different values of γ_H and γ_L are given

Index	1	2	3	4	5	6	7	8	9	10	11
γ_H, γ_L	0.6, 0.5	0.7, 0.5	0.8, 0.5	0.9, 0.5	1, 0.2	1, 0.3	1, 0.4	1, 0.5	1, 0.8	1.5, 0.5	1.5, 0.8

traditional Laws' mask has achieved the classification accuracy of 98.50% for the mean filter, 97.33% for the absolute mean filter and 96.67% for the standard deviation filter. For ALOT dataset the proposed homomorphic normalized Laws' mask approach for the mean filter has provided the highest classification accuracy of 99.17% at value of $\gamma_H = 1$ and $\gamma_L = 0.5$. The second best classification rate of 99.00% is achieved with two different values, i.e. at $\gamma_H = 0.8$ and $\gamma_L = 0.5$, and at $\gamma_H = 0.7$ and $\gamma_L = 0.5$ for the mean filter. The third highest classification accuracy of 98.83% is attained at two different values, i.e. at $\gamma_H = 1$ and $\gamma_L = .2$, and at $\gamma_H = 1$ and $\gamma_L = .8$ for the mean filter. For the standard deviation filter higher classification accuracy of 97.00% is obtained at the value $\gamma_H = 1$ and $\gamma_L = 0.5$. There is no increment in the classification rates for the absolute mean filter on this dataset. The conventional co-occurrence approach has delivered classification accuracy of 87.00% on ALOT database. Among all the proposed homomorphic normalized co-occurrence approach the highest classification accuracy of 91.00% is obtained at $\gamma_H = 0.8$ and $\gamma_L = 0.5$. The second highest classification accuracy of 90.33% is obtained for value at $\gamma_H = 1$ with different values of γ_L, i.e. $\gamma_L = 0.2, 0.3, 0.4$. The third highest classification accuracy of 90.13% is achieved at value of $\gamma_H = 0.7$ and $\gamma_L = 0.5$.

It is observed that maximum increment of 5% for the mean filter, 11% for the absolute mean filter, and 12.5% for the standard deviation filter are attained on STex dataset. For VisTex dataset maximum increment in classification rates are 5.5% for the mean filter, 7.5% for the absolute mean filter, and 7% for the standard deviation filter. For ALOT dataset maximum increment in classification accuracies are 0.67% for the mean filter and 0.33% for the standard deviation filter. All these results discussed above are obtained by employing the normalized Laws' mask descriptor. By utilizing the normalized co-occurrence approach the maximum increment in classification accuracies are of 19.5% on STex, 7% on VisTex, and 4% on ALOT datasets. These results corroborate the robustness in texture description of the proposed method since these datasets present several challenges, such as a high number of classes, viewpoint and illumination changes. Tables 1, 2, 3 and 4 present the results discussed above. The graphical presentation of classification accuracies for conventional co-occurrence and Laws' mask descriptors are shown in Figs. 6 and 7. The graphical presentation of classification accuracies of homomorphic normalized descriptors is given from Figs. 8, 9, 10 and 11. Table 5 presents the value of γ_H and γ_L according to which the graphs of normalized descriptors are plotted.

5 Conclusion

We have introduced a new illumination normalized colour texture analysis method that combines the homomorphic filter with Laws' mask and co-occurrence descriptor for texture classification. We have discussed the concept of RGB space and parameter selection of DoG filter used in homomorphic filter. Experiments on three commonly used datasets indicate that the suggested approaches have considerably enhanced the classification rates with respect to the traditional methods. Thus, the proposed method proves the robust performance of illumination normalization in colour texture analysis. For future work, artificial neural network can be considered in the task of classification.

References

1. Tan, T.S.C.; Kittler, J.: Colour texture analysis using colour histogram. IEEE Proc. Vis. Image Signal Proces **141**(6), 403–412 (1994)
2. Kyllonen, J.; Pietikainen, M.: 5-1 Visual inspection of parquet slabs by combining color and texture. In: Proceedings of IAPR Workshop on Machine Vision Applications (MVA'00). November 28–30, Tokyo, Japan. pp. 187–192 (2000). http://citeseerx.ist.psu.edu/viewdoc/summary?doi=10.1.1.145.4457
3. Drimbarean, A.; Whelan, P.F.: Experiments in colour texture analysis. Patt. Recogn. Lett. **22**, 1161–1167 (2001). https://doi.org/10.1016/S0167-8655(01)00058-7
4. Palm, C.; Lehmann, T.M.: Classification of colour textures by Gabor filtering. Mach. GRAP. Vis. **11**(2/3), 195–219 (2002). https://doi.org/10.1109/34.41384
5. Palm, C.: Colour texture classification by integrative co-occurrence matrices. Patt. Recogn. **37**, 965–976 (2004). https://doi.org/10.1016/j.patcog.2003.09.010
6. Arivazhagan, S.; Ganesan, L.; Angayarkanni, V.: Color texture classification using WSFs and WCFs. Multi. Cyperscape J.-Special Iss. Mult. Data Proc. Comp. **3**(4), 297–302 (2005). https://doi.org/10.1109/ICCIMA.2005.46
7. Arivazhagan, S.; Ganesan, L.; Joyson, C.T.: Color texture image classification using wavelet texture spectral features. Int. J. Biomed. Eng. Consum. Health Inform. **3**(1), 21–27 (2011). ISSN: 0973-6727.
8. Dey, M.; Raman, B.; Verma, M.: A novel colour-and texture-based image retrieval technique using multi-resolution local extrema peak valley pattern and RGB colour histogram. Pattern Anal. Appl. **19**(4), 1159–1179 (2016)
9. Haralick, R. M.: Statistical and structural approaches to texture. In: Proceedings of IEEE (Vol. 67, pp. 786–804). (1979). https://doi.org/10.1109/proc.1979.11328

10. Laws, K.I.: Texture energy measures. In: Image Und. Workshop. (1979).
11. Ojala, T.; Pietikainen, M.; Maenpaa, T.: Multi resolution gray-scale and rotation invariant texture classification with local binary patterns. IEEE Trans. Pattern Anal. Mach. Intell. **24**, 971–987 (2002). https://doi.org/10.1109/TPAMI.2002.1017623
12. Unser, M.: Texture classification and segmentation using wavelet frames. IEEE Trans. Image. Process. **4**(11), 1549–1560 (1995). https://doi.org/10.1109/83.469936
13. Manjunath, B.S.; Ma, W.Y.: Texture features for browsing and retrieval of large image data. IEEE Trans. Patt. Anal. Machine Intell. **18**(8), 837–849 (1996). https://doi.org/10.1109/34.531803
14. Arivazhagan, S.; Ganesan, L.: Texture classification using wavelet transform. Patt. Recogn. Lett. **24**(9–10), 1513–1521 (2003). https://doi.org/10.1016/S0167-8655(02)00390-2
15. de Siqueira, F.R.; Schwartz, W.R.; Pedrini, H.: Multi-scale gray level co-occurrence matrices for texture description. Neurocomputing **120**, 336–345 (2013). https://doi.org/10.1016/j.neucom.2012.09.042
16. Yadav, A.R.; Anand, R.S.; Dewal, M.L.; Gupta, S.: Multiresolution local binary pattern variants based texture feature extraction technique for efficient classification of microscopic images of hard wood species. App. Soft Comp. **32**, 101–112 (2015). https://doi.org/10.1016/j.asoc.2015.03.039
17. Yadav, A.R.; Anand, R.S.; Dewal, M.L.; Gupta, S.: Gaussian image pyramid based texture features for classification of microscopic images of hardwood species. Optik. **126**(24) 5570–5578 (2015). https://doi.org/10.1016/j.ijleo.2015.09.030.
18. Dash, S.; Jena, U.R.: Texture classification using steerable pyramid based Laws' masks. J. Elect. Syst. Inform. Tech. **4**, 185–197 (2017). https://doi.org/10.1016/j.jesit.2016.10.001
19. Du, S.; Ward, R.: Wavelet-based illumination normalization for face recognition. In: IEEE International Conference on Image Processing (ICIP 2005), Vol. 2, (2005). https://doi.org/10.1109/ICIP.2005.1530215
20. Jobson, D.J.; Rahman, Z.; Woodell, G.A.: A multiscaleretinex for bridging the gap between color images and the human observation of scenes. IEEE Trans. Image. Proc. **6**(7), 965–976 (1997). https://doi.org/10.1109/83.597272
21. Delac, K.; Grgic, M.; Kos, T.: Sub-image homomorphic filtering technique for improving facial identification under difficult illumination conditions. In: International Conference System, Signals and Image Processing pp. 95–98 (2006). http://citeseerx.ist.psu.edu/viewdoc/download?doi=10.1.1.118.1579&rep=rep1&type=pdf
22. Wang, W.; Song, J.; Yang, Z.; Chi, Z.: Wavelet-based illumination compensation for face recognition using eigenface method. In: Proceedings 6th World Congress Intelligent Control and Automation, Dalian, China (2006). https://doi.org/10.1109/WCICA.2006.1714031
23. Chen, W.; Joo Er, M.; Wu, S.: Illumination compensation and normalization for robust face recognition using discrete cosine transform in logarithm domain. IEEE Trans. Syst. Man Cybern. **36**(2), 458–466 (2006). https://doi.org/10.1109/TSMCB.2005.857353
24. Xie, X.; Lam K-N.: An efficient illumination normalization method for face recognition. Patt. Recg. Lett. **27**, 609–617 (2006). https://doi.org/10.1016/j.paterc.2005.09.026
25. Emadi, M.; Khalid, M.; Yusof, R.; Navabifar, F.: Illumination normalization using 2D Wavelet. Procedia Eng. **41**, 854–859 (2012). https://doi.org/10.1016/j.proeng.2012.07.254
26. Tan, X.; Triggs, B.: Enhanced local texture feature sets for face recognition under difficult lighting conditions. IEEE Trans. Image Proc. **19**(6), 1635–1650 (2010). https://doi.org/10.1109/TIP.2010.2042645
27. Fan, C.N.; Zhang, F.Y.: Homomorphic filtering based illumination normalization method for face recognition. Patt. Recog. Lett. **32**, 1468–1479 (2011). https://doi.org/10.1016/j.patrec.2011.03.023
28. Maenpaa, T.; Pietikainen, M.: Classification with color and texture: jointly or separately? Patt. Recogn. **37**(8), 1629–1640 (2004). https://doi.org/10.1016/j.patcog.2003.11.011
29. Burghouts, G.J.; Geusebroek, J.M.: Material-specific adaption of colour invariant features. Patt. Recgon. Lett. **30**, 306–313 (2009). https://doi.org/10.1016/j.patrec.2008.10.005
30. Vacha, P.; Haindl, M.: Texture recognition using robust Markovian features. In: International Workshop on Computational Intelligence for Multimedia Understanding. Springer, Berlin, pp. 126–137 (2012). https://doi.org/10.1007/978-3-642-32436-9-11
31. Kononenko, I.; Kukar, M.: Machine learning and data mining: introduction to principles and algorithms. Horwood Publishing Ltd, Chichester (2007)
32. Everitt, B.S.; Landau, S.; Leese M.; Stahl, D.: Miscellaneous clustering methods. In Cluster Analysis. Wiley Series in Probability and Statistics. Wiley, New York, pp. 215–255 (2011). https://doi.org/10.1002/9780470977811.ch8
33. Hastie, T.; Tibshirani R.; Friedman, J.: The elements of statistical learning. Springer series in statistics, New York, Vol. 1, pp. 241–249, (2009). https://doi.org/10.1007/978-0-387-84858
34. Department of Computer Sciences, U. S., Salzburg texture image database (STex), http://www.wavelab.at/sources/STex/.
35. VisTex, Texture dataset, http://vismod.media.mit.edu/vismod/imagery/VisionTexture/vistex.html.
36. Amsterdam library of textures (ALOT), http://www.science.uva.nl/~mark/ALOT.